CSIRO PUBLISHING

International Journal of Wildland Fire **2017**, *26*, 844
https://doi.org/10.1071/WF16032

Retraction notice to 'Projected changes in Australian fire regimes during the 21st century and consequences for ecosystems.' [*International Journal of Wildland Fire* (2016) doi: 10.1071/WF16032]

S. P. Harrison[A,B,C] *and D. I. Kelley*[A,B]

[A]School of Biological Sciences, Macquarie University, North Ryde, NSW 2109, Australia.
[B]School of Archaeology, Geography and Environmental Science, Reading University, Whiteknights, Reading, RG6 6AH, UK.
[C]Corresponding author. Email: s.p.harrison@reading.ac.uk

Refers to: RETRACTED: Projected changes in Australian fire regimes during the 21st century and consequences for ecosystems

International Journal of Wildland Fire, published online September 2016, doi.org/10.1071/WF16032. S. Harrison and D. I. Kelley

After due consideration, the editors of the journal agree that the paper be retracted from *International Journal of Wildland Fire*.

Reason: While this paper adds valuable new data and analysis to a previously published paper (Kelley DI, Harrison SP (2014) Enhanced Australian carbon sink despite increased wildfire during the 21st century. *Environmental Research Letters* **9** 104015. doi:10.1088/1748-9326/9/10/104015), the 2014 paper was not cited. As a result, the objectives, results and conclusions of this research were not differentiated from those in the 2014 publication.

CSIRO PUBLISHING

International Journal of Wildland Fire
https://doi.org/10.1071/WF16032

Projected changes in Australian fire regimes during the 21st century and consequences for ecosystems

S. P. Harrison[A,B,C] *and D. I. Kelley*[A,B]

[A]School of Biological Sciences, Macquarie University, North Ryde, NSW 2109, Australia.
[B]School of Archaeology, Geography and Environmental Science, Reading University, Whiteknights, Reading, RG6 6AH, UK.
[C]Corresponding author. Email: s.p.harrison@reading.ac.uk

Abstract. Climate projections show Australia becoming significantly warmer during the 21st century while precipitation decreases over much of the continent. Such changes are generally considered to increase wildfire risk. Nevertheless, using a process-based model of vegetation dynamics and vegetation–fire interactions, we show that while burnt area increases in southern and central Australia, it decreases in northern Australia. Overall, the projected increase in fire by the end of the 21st century is small (0.7–1.3% of land area, depending on the climate scenario). The direct effects of increasing CO_2 on vegetation productivity and water-use efficiency influence simulated fire regimes: CO_2 effects tend to increase burnt area in arid regions, but increase vegetation density and reduce burnt area in forested regions. Increases in burnt area promote a shift to more fire-adapted trees in wooded areas and their encroachment into grasslands, with an overall increase in forested area of 3.9–11.9% of land area by the end of the century. The decrease in burnt area in northern Australia leads to an increase in tree cover (~20%) and an expansion of tropical forest. Thus, although the overall change in burnt area is small, it has noticeable consequences for vegetation patterns across the continent.

Additional keywords: biome shifts, CO_2 impacts on fire, fire dampening-induced vegetation changes, fuel limitation, resprouting vegetation.

Received 3 October 2015, accepted 6 August 2016, published online 12 September 2017

Introduction

Approximately 5% (0.41×10^6 km^2) of the Australian continent burns annually, and all but the most arid parts of the continent are susceptible to periodic fire (Bradstock *et al.* 2012; Hughes and Steffen 2013; Murphy *et al.* 2013). Fire frequency is particularly high in the tropical savannas of northern Australia (1–5 years) although the intensity of these fires is low, whereas more intense but less frequent (>100 years) fires are characteristic of the forests of eastern Australia. Fires are more frequent (1–10 years) in woodlands in the continental interior, but become increasingly rare towards the arid regions because of fuel limitation (Murphy *et al.* 2013). Much of the Australian vegetation is adapted to fire through strategies that promote rapid re-establishment from seed or recovery through resprouting (Lawes *et al.* 2011; Bradstock *et al.* 2012; Clarke *et al.* 2013). Nevertheless, changes in fire regimes are of concern both because of the rapidly escalating social and economic costs (Ashe *et al.* 2008; Crompton and McAneney 2008; Stephenson *et al.* 2012; Hughes and Steffen 2013) and because of the potential impacts on vegetation and biodiversity (Bradstock 2008; Williams *et al.* 2009; Gill 2012).

Climate projections for the 21st century (Collins *et al.* 2013; Kirtman *et al.* 2013) show significant warming over Australia, with decreased precipitation in many regions. Warmer and drier conditions are generally considered to increase in the risk of fire in Australia (Williams *et al.* 2001; Hennessy *et al.* 2005; Lucas *et al.* 2007; Pitman *et al.* 2007; Fox-Hughes *et al.* 2014). However, increased fire risk does not necessarily translate into increased burning in situations where the climate changes reduce vegetation productivity and hence fuel loads (Harrison *et al.* 2010; Bistinas *et al.* 2014; Higuera *et al.* 2015; Knorr *et al.* 2016*a*, 2016*b*). Indeed, statistical modelling suggests either a reduction (Krawchuk *et al.* 2009) or only a moderate increase (Moritz *et al.* 2012) in fire activity in Australia. The reliability of these projections is compromised because they do not account for the impact of changing CO_2 concentrations on vegetation productivity and water-use efficiency or for potential changes in vegetation distribution and their impact on fire regimes under a changing climate. Both of these effects are included in process-based dynamic global vegetation models (DGVMs).

Here, we use a version of the Land surface Processes and eXchanges Dynamic Global Vegetation Model (LPX-Mv1 DGVM; Kelley *et al.* 2014) driven by outputs from nine coupled ocean–atmosphere models forced using two different future scenarios of changes in atmospheric composition and land use from the fifth phase of the Coupled Model Intercomparison Project (CMIP5; Taylor *et al.* 2012) to examine potential changes in Australian fire regimes over the 21st century and the implications of these changes for natural vegetation patterns.

Methods

Study area

Australia spans 29° of latitude, with a temperature gradient from tropical in the north to temperate in the south. Much of the continent is arid or semiarid. Precipitation regimes reflect the seasonal migration of the subtropical anticyclone belt (Sturman and Tapper 2005). Most of the north is influenced by south-easterly trade winds in winter and monsoonal flow in summer, and hence has highly seasonal rainfall, with dry winters and wet summers. The central interior, dominated by travelling anticyclones throughout the year, is dry. Troughs between the travelling anticyclones entrain maritime north-westerly airflows, bringing summer rain to parts of the east coast and southern highlands. Southern Australia, dominated by travelling anticyclones in summer and westerly winds in winter, has winter rainfall and dry summers. Much of northern and eastern Australian experiences considerable interannual variability in precipitation, associated with the El Nino–Southern Oscillation.

The natural vegetation of Australia follows a structural continuum reflecting these rainfall patterns (Groves 1994). Closed forests are distributed discontinuously along the east coast from north-eastern Queensland to western Tasmania, in regions with year-round rainfall. Tall, open forests occur throughout coastal and montane south-eastern Australia and in south-western Australia, in subhumid sites with either summer or winter rainfall. Woodlands occupy drier areas inland, wherever rainfall is sufficient regardless of source or season. Mallee shrubland occurs in areas of southern Australia with a long dry season but where westerly flow brings rain in winter. The arid interior is largely characterised by shrubland and tussock grass.

Fire plays a major role in shaping Australian vegetation patterns, and many plants show adaptations to fire (Law *et al.* 2011; Bradstock *et al.* 2012; Clarke *et al.* 2013). The different climate regimes and vegetation types give rise to different fire regimes across the continent (Murphy *et al.* 2013). Most of the closed forests in eastern Australia burn infrequently, but when fires do occur in hot, dry years, the abundance of fuel leads to high-intensity ground and crown fires. In the continental interior, aridity prevents the build-up of high fuel loads, limiting both the occurrence and intensity of fire. The seasonal precipitation regime in northern Australia allows fuel accumulation in the wet season and promotes rapid drying in winter. This results in frequent fires, but their regularity inhibits fuel build-up and thus these fires are generally of low intensity. Seasonal precipitation regimes in southern Australia are often characterised by high interannual variability, and this leads to more unpredictable fire seasons than in northern Australia. The role of fuel loads in creating the diversity of fire regimes across the continent provides a major justification for using process-based modelling to investigate the impacts of climate change on fire regimes.

The model and modelling approach

We use the LPX-Mv1 fire-enabled DGVM (Kelley *et al.* 2014) to simulate the response of Australian fire regimes and vegetation to climate changes resulting from two scenarios of 21st century changes in atmospheric composition and land use. We use outputs from multiple coupled ocean–atmosphere models driven by these two scenarios to encompass the range of potential responses to each scenario. LPX-Mv1 (Kelley *et al.* 2014) was developed from the LPX DGVM (Prentice *et al.* 2011); the vegetation dynamics component of LPX was based on the Lund–Potsdam–Jena (LPJ) DGVM (Sitch *et al.* 2003). The model simulates vegetation and fire properties on a spatial grid of 0.5° by 0.5°; it does not simulate spatially explicit distributions within a grid cell.

Vegetation within a grid cell is described in terms of fractional coverage of plant functional types (PFTs), defined by life form (tree, grass), with grasses further subdivided by photosynthetic pathway (C_3, C_4) and trees by bioclimatic tolerance (tropical, temperate, boreal), leaf type (broadleaf, needleleaf), and phenological response to drought or cold (evergreen or deciduous). LPX-Mv1 differs from LPX by including resprouting and non-resprouting variants of tropical broadleaf evergreen trees, tropical broadleaf deciduous trees, temperate broadleaf evergreen trees and temperate broadleaf deciduous trees. Climatic tolerance limits determine whether a PFT could occur in a grid cell. Establishment rates are dependent on the area available for colonisation, except that resprouting PFTs have lower establishment rates than non-resprouting PFTs. The abundance of each PFT is determined through competition, as a function of PFT-specific productivity. Gross primary production is calculated for each PFT using an explicit photosynthesis model and detailed accounting of the water and energy exchanges between vegetation and the atmosphere (Sitch *et al.* 2003). Transpiration, and therefore gross primary production (GPP), is limited if available water is less than the maximum demand. Atmospheric CO_2 concentration affects the water cost per unit production. Primary Production (NPP) is calculated after accounting for maintenance and growth respiration, and allocated in fixed proportions to roots, leaves and woody tissues.

The dynamic vegetation component of the model provides information on vegetation type and productivity that is then used to specify fuel loads in the fire component of the model. Woody material contributes to coarse fuel, while leaves and grass contribute to fine fuel loads (Fig. 1). The soil moisture accounting scheme in the vegetation component is used to predict the moisture content of live fuel. Vegetation information is passed to the fire module once a year.

The fire module in LPX-Mv1 represents the influence of potential ignition rates, vegetation properties and weather conditions on biomass burning through explicit formulations of the probability of fires starting, their rate of spread, fire intensity and the amount of fuel combusted, and the consequences for the mortality and regeneration of different PFTs. The model simulates multiple aspects of the fire regime (number of fires, fire type, intensity, frequency and burnt area), and changes in these characteristics influence vegetation composition.

Fire is explicitly simulated in each grid cell on a daily timestep. This temporal resolution means that the model is adapted to using daily mean climate conditions as inputs; it does not take account of sub-daily or short-lived extreme conditions such as wind gusts. The number of fire starts is a function of lightning ignitions and fire susceptibility (Fig. 1). LPX-Mv1 does not include human ignitions. Although human ignitions affect the number and seasonality of fires (Russell-Smith *et al.* 2007; Archibald *et al.* 2013), they have little effect on burnt area (Bistinas *et al.* 2014; Knorr *et al.* 2014; Knorr *et al.* 2016*a*).

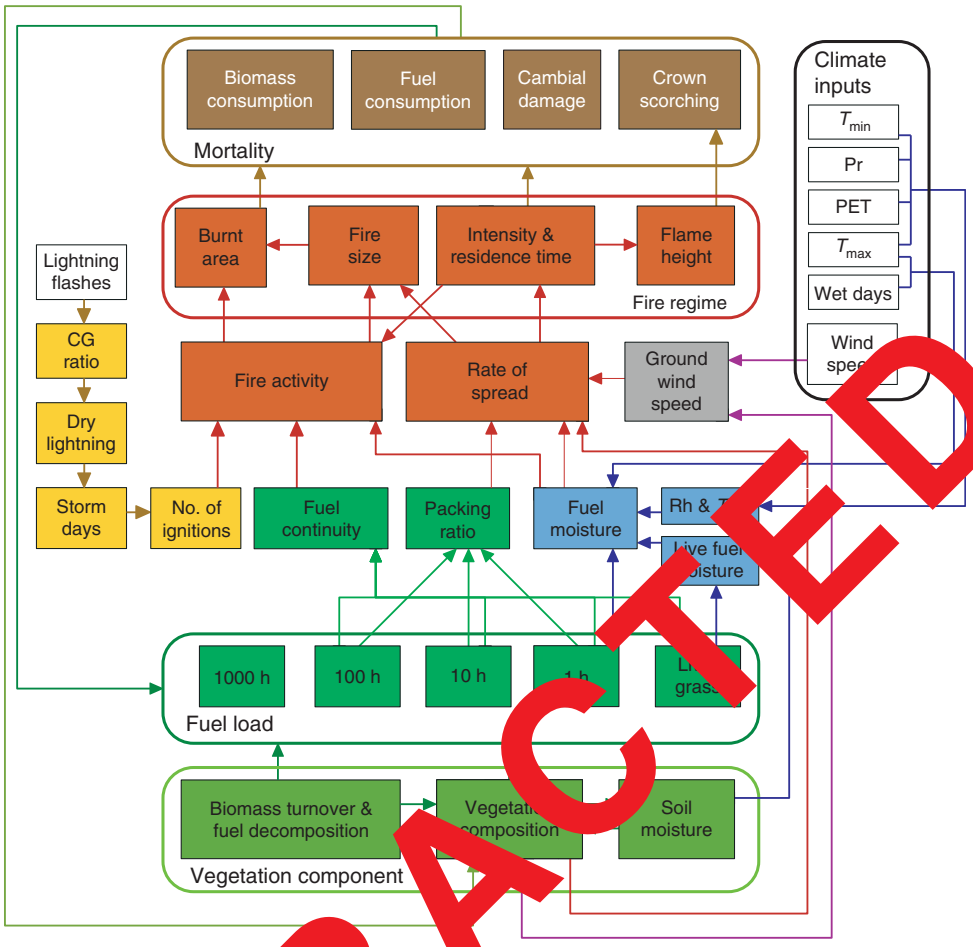

Fig. 1. Description of the st ure of t omponent of LPX-Mv1. Climate and lightning inputs to the model are identified by white boxes, o ts th tation dynamics component of the model are identified by green boxes. The climate an ghtning ts are monthly values of: minimum temperature (Tmin), precipitation (Pr), potential evapotran ation (PET), m mum temperature (Tmax), number of wet days (Wet days), surface wind speed (Wind sp the total numb r of lightning flashes from which the number of cloud to ground (CG) flashes is deter ined. ternal processes and exchanges that are explicitly simulated by the fire component of the model re colour-code ere pale green boxes show state variables associated with fuel load, blue boxes show state v oles associated wit uel moisture (where Rh is relative humidity and Tdew is dewpoint temperature), yell boxes w state variables associated with ignitions, red boxes show state variables associated with fire reg an rown b xes show state variables associated with mortality and biomass consumption.

LPX-Mv lows fraction of ground strikes to vary spatially and sea ally rea ically partitions strike distribution between we dry days, and has a variable number of strikes on dry days (y *et al.* 2014). Fire susceptibility takes into account the amount, properties and moisture content of the available fuel load. There are four fuel size classes: 1-h or fine fuel (derived from leaves and grass), 10-h (from small branches), 100-h (from large branches) and 1000-h (from boles and trunks) fuels. The size class determines the rate at which fuel moisture equilibrates to relative humidity on dry days. Ignitions do not result in a fire unless the combined load of 1-, 10- and 100-h fuel is greater than 200 g m^{-2}, a surrogate for minimal fuel continuity (Thonicke *et al.* 2001). Fuel loads can be reduced through fire or decomposition, where coarse and fine fuels decompose at different rates (Brovkin *et al.* 2012).

Fire spread, intensity and residence time are dependent on wind speed and fuel moisture (Fig. 1), and calculated using the Rothermel equations (Rothermel 1972). Fires are assumed to be elliptical and fire size is therefore calculated using a simple geometric relationship with rate of spread. Wind speed is modulated by vegetation type and density, as measured by foliar projective cover. Burnt area is calculated as the product of the number of fires and fire spread.

Mortality occurs through crown scorching and cambial death, where cambial damage is determined by fire intensity and residence time in relation to the bark thickness of woody vegetation. In LPX-Mv1, the PFT-specific bark thickness is specified as a range when new populations establish. Fires will preferentially remove thin-barked trees, leading to a change in average bark thickness as a consequence of fire history (Kelley

Table 1. Summary of the simulation protocol for model spin-up and the simulations
CRU TS3.1, Climate Research Centre Time Series 3.1 (CRU TS3.1) dataset; NCEP, National Center for Environmental Prediction reanalysis data set; LIS-OTD, High Resolution Monthly Climatology of lightning flashes from the Lightning Imaging Sensor–Optical Transient Detector

Period	CO_2	Maximum and minimum temperature, precipitation, rain days, and sunshine hours	Wind speed	Lightning
Spin-up	286 ppm	Detrended CRU TS3.1	Detrended NCEP	Climatology LIS-OTD
1850–1900	Transient	Detrended CRU TS3.1	Detrended NCEP	Climatology LIS-OTD
1901–1947	Transient	Transient CRU TS3.1	Detrended NCEP	Climatology LIS-OTD
1948–1979	Transient	Transient CRU TS3.1	Transient NCEP	Climatology LIS-OTD
1980–2006	Transient	Transient CRU TS3.1	Transient NCEP	Climatology LIS-OTD
2006–2100	Transient	Transient	Transient	Climatology LIS-OTD

et al. 2014). Resprouting PFTs survive fires if there is unconsumed aboveground biomass; plant size and productivity after resprouting are, however, reduced in proportion to the amount of biomass consumed.

Given its spatial and temporal resolution, LPX-Mv1 is particularly well adapted to simulate regional-scale changes in burnt area, the aspect of the fire regime that is important for carbon cycle and climate feedbacks, in response to changes in climate. The 21st century LPX-Mv1 simulations are idealised experiments focusing on the impact of climate and CO_2 changes on vegetation and fire regimes. They do not account for potential future changes in the number of lightning strikes or in anthropogenic fire suppression. There is no convincing evidence f changes in thunderstorm frequency over the late 20th century (Hartmann *et al.* 2013) and estimates of the change in lightning flash rate with future warming vary considerably illiams 1992; Price and Rind 1994; Michalon *et al.* 1999 omp *et al.* 2014). Furthermore, sensitivity analyses sho at cha the number of strikes have relatively little effec nt ar compared with the impact of changing w er condi s on the probability that a strike will cause ig (Kelley *et a* 014). Anthropogenic landscape fragmen ion nificantly reduces fire spread and hence burnt area (Bistinas *et a* 014; Knorr *et al.* 2014) but is not included in th 1st century sim ations because projected changes in land are highly uncertain.

Input data

The daily clima required he fire module are calculated in the m el by r interpolation between the monthly values for ea ari as ed to the midpoint of each month. Monthly maxim and minimum temperature, precipitation, cloud cover, and n ber of wet days were obtained from the Climate Research Centre Time Series 3.1 (CRU TS3.1) dataset (Harris *et al.* 2013) and monthly wind speed from the National Center for Environmental Prediction (NCEP) reanalysis dataset (Kalnay *et al.* 1996). The model includes a weather generator (Geng *et al.* 1988) that allocates precipitation to wet days taking account of persistence in dry and wet conditions, and distributes the observed monthly precipitation to wet days using an empirically based function of rainfall distribution such that the amount of rain falling on each wet day is different. A seasonal climatology of lightning ignitions is calculated from the High-Resolution Monthly Climatology of lightning flashes from the Lightning Imaging Sensor ptical Transie Detector (LIS/OTD) dataset (availab at p://gcmd.nasa.gov/records/GCMD_lohrmc.html acces 6 Aug 2016). Atmospheric CO_2 concentratio prescri ally as a single global value from obse ns (availabl http://www.esrl.noaa.gov/gmd/, accesse 16 A st 2016).

The model was sp up (Table 1) using constant CO_2 (286 p d detrended limate data until the carbon pools were equilibrium. The detrended climate data were obtained by r essing th nnual average values for all climate variables for t eriod 1 0–2000 on each grid cell and removing the value es or the slope of this regression from the monthly ata. The historical run (Table 1) used transient CO_2 from 1850 o . The detrended climate data were used until time-ying data were available, i.e. after 1948 for wind speed and rom 1901 onwards for all other climate variables (Table 1).

LPX-Mv1 was run from 2006 to 2100 using climate realisations from nine coupled ocean–atmosphere climate models (Table 2) forced by two alternative Representative Concentration Pathway (RCP) scenarios (van Vuuren *et al.* 2011): RCP4.5 and RCP8.5. Lightning ignitions are prescribed as in the historic simulation. However, because the number of dry-day strikes is determined by number of wet days per month, the interannual variability in the number of dry strikes is different in the future simulations from in the historic period. LPX-Mv1 is also driven by atmospheric CO_2, which changes in the RCP4.5-driven simulations from 380.8 to 576 ppm by 2080 CE and stabilises thereafter. In the RCP8.5 simulations, CO_2 concentrations increase continuously to reach 1231 ppm by 2100. To examine the direct impact of increasing CO_2 on vegetation productivity and water-use efficiency, we made additional simulations in which climate varied but CO_2 was held constant at the 2006 level of 380.8 ppm (fixed-CO_2 experiment).

Model evaluation

The historic simulation was evaluated by comparing simulated and observed vegetation distribution (DeFries and Hansen 2009), fine litter production, as a surrogate for fuel load (Vegetation And Soil-carbon Transfer (VAST) dataset: Barrett 2001), carbon (Ruesch and Gibbs 2008), and burnt area and timing of the fire season from the 4th version of the Global Fire Emissions Data (GFED4; Giglio *et al.* 2013). The simulations do not take account of land-use changes, so cropland areas were

Table 2. Information on the models used to provide future climate scenarios

OA models are coupled ocean–atmosphere models; OAC models include a marine and terrestrial carbon cycle. The resolution (number of grid cells by latitude and longitude) is that of the atmospheric and land-surface components of each model

Code	Centre	Type	Original resolution
CNRM-CM5	Centre National de Recherches Meteorologiques	OA	128, 256
GISS-CM5	NASA Goddard Institute for Space Studies	OA	90, 144
HadGEM2-CC	Hadley Centre, UK Meteorological Office	OA	145, 192
MRI-CGCM3	Meteorological Research Institute	OA	160, 320
HadGEM2-ES	Hadley Centre, UK Meteorological Office	OAC	145, 192
IPSL-CM5a-LR	Institut Pierre-Simon Laplace	OAC	
MIROC-ESM	Japan Agency for Marine–Earth Science and Technology	OAC	4, 12
MPI-ESM-LR	Max Planck Institute for Meteorology	OAC	96, 192
BCC-CSM1–1	Beijing Climate Centre	OAC	4, 128

Table 3. Benchmarking metrics for the modern simulation of Aus lian v tion a ire

The Manhattan Metric (MM) is used to assess vegetation properties, the normalised m error (NM ss fine fuel loads, burnt area and carbon, and the mean phase difference (MPD) to assess fire seasonality. V r the mean an ndom null model for each variable are given for comparison. Values that are better than the mean null mo are s in italics, values that are better than the random null model are indicated by an asterisk. n/a, not a able

	Tree cover	Grass cover	Fin el	Burnt area	Fire season	Carbon
Observed mean	8.4%	65%	230 $^{-2}$	6	n/a	2388 g C m^{-2}
Simulated mean	4.9%	55%	202 g	5 %	n/a	3481 g C m^{-2}
Metric	MM	MM	NME	ME	MPD	NME
Mean null model	0.43	0.49		1	0.45	1
Random null model	0.52 ± 0.002	0.66 ± 10.002	1. 31	1.14 ± 0.003	0.47 ± 0.002	1.19 ± 0.013
LPX-Mv1 mean	*0.16**	0.51*	*	*0.88**	*0.43**	*0.94**

masked out (using the Global Land Cover (GLC2000) 5 × 5′ land-cover map; Bartholo and Be 2005) in making these comparisons.

We used benchmarking metrics here performance is expressed relative to a mea and random del for each variable (Kelley *et al.* 2013) to uate the realism of the simulations. We use the norma d m error (NME) to account for geographic patterning parison of total values and annual averages; these scores p de a scription of the spatial error of the mod le 3). NME takes the value 0 when agreeme perf 1 when agreement is equal to that expected when th an ue all observations is substituted for the model, and es >1 when the model's performance is worse than the null el. We use the Manhattan Metric (MM) for measures of relative abundance (i.e. where the sum of items in each grid cell must be equal to 1, e.g. for vegetation cover). MM takes the value 0 for perfect agreement, and 2 for complete disagreement. Temporal differences in the timing of the fire season were assessed by calculating the mean phase difference (MPD, Table 3) in months between observation and simulations, where 0 indicates perfect agreement and 1 perfect disagreement in timing.

Two null models were constructed for each benchmark to facilitate interpretation of the metric scores (Table 3). The 'mean null model' compares each benchmark with a dataset of the same size, filled with the mean of the observations. The 'random null model' is constructed by creating a dataset of the same dimensions as the benchmark dataset by bootstrap resampling of the observations, using 1000 randomisations to estimate a probability density function of the scores.

Analyses of future fire

We examine the 21st century changes in vegetation and fire, focusing on burnt area, for the continent as a whole and for regions where there is a consistent signal in the direction of the simulated change in burnt area during the 21st century. We defined four regions for this second analysis: northern Australia (north of 17°S), central Australia (between 24° and 35°S and 124° and 148°E), south-eastern Australia (the area lying to the south-east of the line joining 32°S 153°E and 38°S 141°E) and south-western Australia (the area south-west of the line joining 25°S 113°E and 33°S 124°E).

Ensemble averages of the LPX-Mv1 outputs were created by simple averaging of the results of individual simulations for each of the RCP scenarios, with and without changes in CO_2 (RCP4.5 varying-CO_2, RCP4.5 fixed-CO_2, RCP8.5 varying-CO_2, RCP8.5 fixed-CO_2). The robustness of the simulated changes is assessed by the agreement between models, while significance is measured by the strength of the change relative to interannual variability in the historic period (1997–2006).

Changes in vegetation are assessed in terms of the abundance of individual PFTs and as shifts in major vegetation types (biomes). We convert the simulated abundance of individual PFTs to biomes using a version of the algorithm described in Prentice *et al.* (2011), in which the boundaries between biomes are defined by the presence and/or absence of specific PFTs and the absolute amounts of tree cover. We define five biomes: grassland and shrubland, sclerophyll woodland, temperate forest, tropical savanna, and tropical forest. We distinguish tropical biomes (tropical savanna, tropical forest) by the presence of either tropical broadleaf evergreen trees or tropical broadleaf deciduous trees. The boundary between shrubland and woodland is set at 2% tree cover and that between woodland and forest at 60% tree cover.

Results

Simulation of present-day vegetation properties and fire regimes

LPX-Mv1 reproduces the observed pattern of tree and grass abundance reasonably well, though there is less woody vegetation in northern Australia and more in south-eastern Australia than observed (Fig. 2; Table 3). Although the model underestimates the amount of woody vegetation (Table 3), transitions from forest through woodland and savanna to grassland in northern and eastern Australia are well captured. LPX-Mv1 reproduces the changing abundance of resprouters and non-resprouters with increasing aridity and post-fire vegetation recovery rates at sites where this has been measured (Kelley *et al.* 2014). Vegetation productivity (NPP) is close to observationally constrained estimates of NPP during the recent decade (Table 3: 2191 Tg C year^{-1} compared with observed values of 2210 ± 398 Tg C year^{-1}: Haverd *et al.* 2013). The model captures the first-order geographic pattern in biomass (Table 3); the largest discrepancies are in areas where tree cover is underestimated. Similarly, the model simulates fine-fuel production comparable with observed values (Table 3: simulated mean 202 g m^{-2} year^{-1} compared with observed mean values of 230 g m^{-2} year^{-1}). Benchmark metrics show LPX-Mv1 performs much better than the null and randomly resampled models for most vegetation properties (Table 3).

LPX-Mv1 reproduces the observed geographic patterns of burnt area reasonably well, in particular the high incidence of fire in northern Australia and more variable levels in the fuel-limited continental interior (Fig. 2). The model overestimates the area burnt in both south-western and south-eastern Australia, and underestimates the burnt area in northern Australia (Fig. 2). Nevertheless, the model correctly predicts the broad-scale patterns in fire seasonality (Table 3), including the prevalence of fires in autumn and winter in northern Australia and in spring and summer in southern Australia. However, there are discrepancies in the timing of peak fire month and fire-season length in central Australia: the timing of the peak fire month can differ by more than 3 months and the fire season can be longer by a similar amount.

Continental response to future climate scenarios

The ensemble average climate shows a robust and significant increase in temperature over the 21st century (Fig. 3) in response to both forcing scenarios. The response to the RCP4.5 scenario is less extreme: the RCP8.5 ensemble average increase in mean annual temperature (MAT) is 4°C by the end of the 21st century, with changes of >5°C in north-western Australia, whereas the RCP4.5 ensemble response is 3°C, although parts of north-western Australia still have increases of >5°C (Fig. 4). The average change in mean annual precipitation (MAP) is small in both scenarios. There is a small but robust and marginally significant decrease in precipitation in northern Australia of ~50 mm year^{-1} in the RCP4.5 scenario runs (Fig. 4), although the decrease can be up to 200 mm year^{-1} in limited areas. Precipitation increases in some regions of the eastern coastal plains, south-eastern Australia and Tasmania, and also south-western Australia, but the changes are small, not robust and not significant. The decrease in precipitation in northern Australia is slightly smaller in the RCP8.5 simulations (~40 mm year^{-1}), although again larger decreases (~125 mm year^{-1}) occur in some places. Changes in MAP over the rest of the country are small, not consistent in sign, and not significant. These climate changes result in an increase in the frequency of 'fire weather', as measured by the cumulative values of the McArthur Mark 5 Forest Fire Danger Index (McArthur 1967; Noble *et al.* 1980) in forest and woodland biomes, and the Grassland Mark 3 Fire Danger Index (McArthur 1966; Pitman *et al.* 2007) in grasslands (Fig. 2, Fig. 3), and drive an overall increase in burnt area.

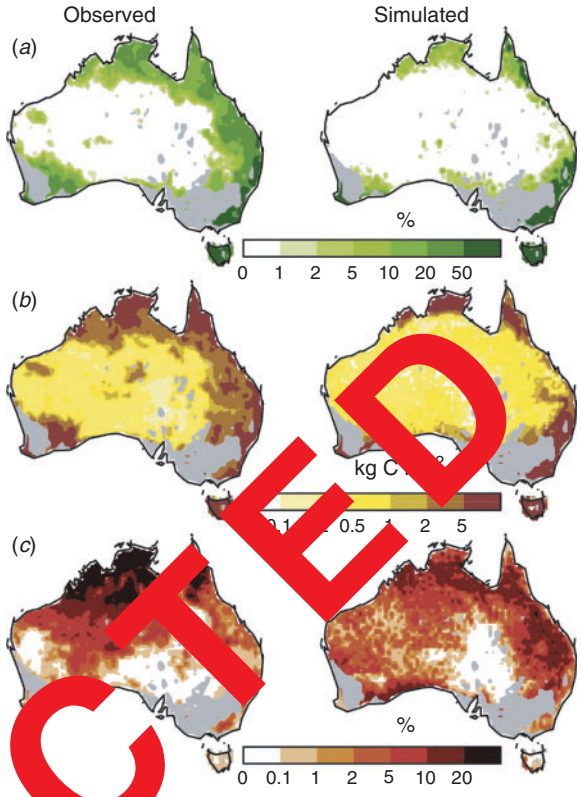

Fig. 2. Comparison of observed (left-hand column) and simulated (right-hand column) vegetation and fire during the recent period. Observed values of tree cover were obtained from DeFries and Hansen (2009). Observed values for (*b*) carbon were obtained from Ruesch and Gibbs (2008). Observed (*c*) average burnt area for the period 1997 to 2006 is from GFED4 (Giglio *et al.* 2013). Grid cells with >50% cropland or urban land are shaded in grey; these cells are not taken into account in the model benchmarking.

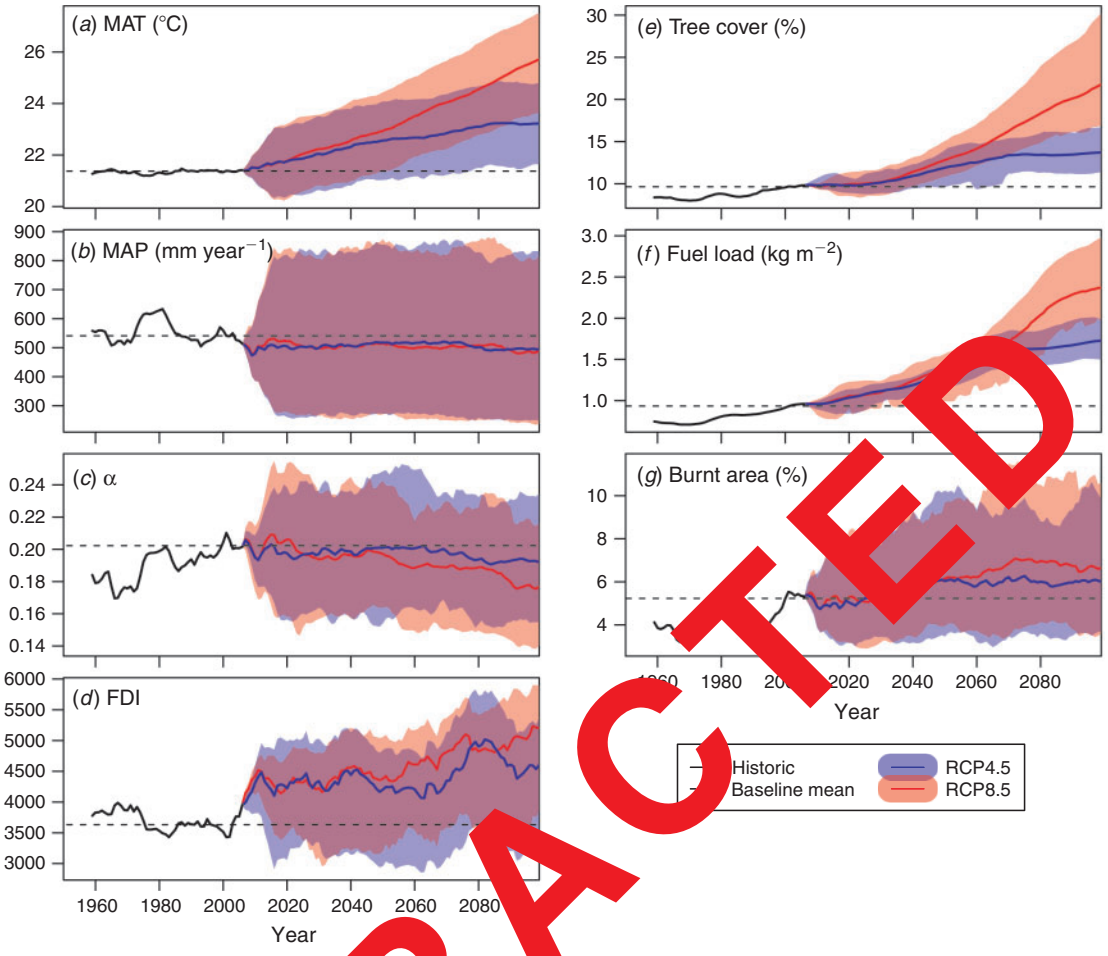

Fig. 3. Changes in climate, fire risk, [illegible]tation [illegible] and burnt area over Australia through the 21st century in simulations driven by the RCP4.5 and RCP8.5 scenarios. The [illegible]ies (bo[illegible]nes) are ensemble averages of the model results, smoothed using a 10-year moving window, where the RC[illegible]5 simulat[illegible]are in blue and the RCP8.5 simulations are in red, for (*a*) mean annual temperature (MAT, °C); (*b*) mean annua[illegible]cipitation (MA[illegible]m year^{-1}); (*c*) the ratio of actual to equilibrium evapotranspiration (α, unitless); (*d*) fire risk as measured [illegible]th[illegible] Arthur cumulative fire danger index (FDI); (*e*) tree cover (%); (*f*) total fuel load (kg m^{-2}); and (*g*) burnt area (%). The range in th[illegible]ividual model simulations is indicated by the shaded bands (red for RCP4.5, blue for RCP8.5). The dashed horizo[illegible]lines indicate [illegible]verage value of each variable during the last decade of the historic simulation.

Nevertheless, the n[illegible] cha[illegible]e in burnt area is only 0.05×10^6 km^2 year^{-1} b[illegible]e en[illegible]f the century in the RCP4.5 simulations[illegible]ly 0.10[illegible]^6 km^2 year^{-1} in the RCP8.5 simulatio[illegible], com[illegible]d with 0.41×10^6 km^2 year^{-1} in the historic sim[illegible]ion[illegible]g.[illegible]Table 4). Thus, the simulated increase is only 12% (R[illegible]4.5) or 24% (RCP8.5) of the historic burnt area. Despite the inc[illegible]e in burnt area, tree cover increases during the century and reaches nearly 22% by the end of the century in the RCP8.5 simulations.

Regional fire regime changes

Despite the decrease in precipitation in northern Australia, there is a significant decrease in burnt area in both the RCP scenarios. Burnt area in northern Australia is reduced from 0.08×10^6 km^2 year^{-1} in the historic simulations to 0.05×10^6 km^2 year^{-1} in the RCP 4.5 simulations and to 0.04×10^6 km^2 year^{-1} in the RCP8.5 simulations (Fig. 5; Table 4), representing a 35% (RCP4.5) or 47% (RCP8.5) decrease in the historic burnt area. Part of the explanation for the decrease is that simulated surface wind speeds decrease during the fire season, limiting fire spread. The reduction in fire is accompanied by an increase in tree cover, from 19% during the historic period to 37% by the end of the 21st century in the RCP4.5 scenario and to 62% by the end of the 21st century in the RCP8.5 scenario. The increase in tree cover leads to a shift in the ratio of fine to coarse fuel: although fuel loads are increased overall, the increase in coarse fuel is larger than the increase in fine fuel (Fig. 5). As a result of this shift, the fuel dries more slowly and this inhibits fire. The increased tree cover reduces rates of fire spread (and hence burnt area) by further decreasing ground wind speed (Rothermel 1972). The increase in tree cover is due to the CO_2-induced increase in C_3 plant water-use efficiency (Fig. 6). Comparison with the fixed-CO_2 simulation shows that climate change alone produces a decrease in tree cover by 10 and 8% in RCP4.5 and RCP8.5 respectively and no significant change in fire (Table 5).

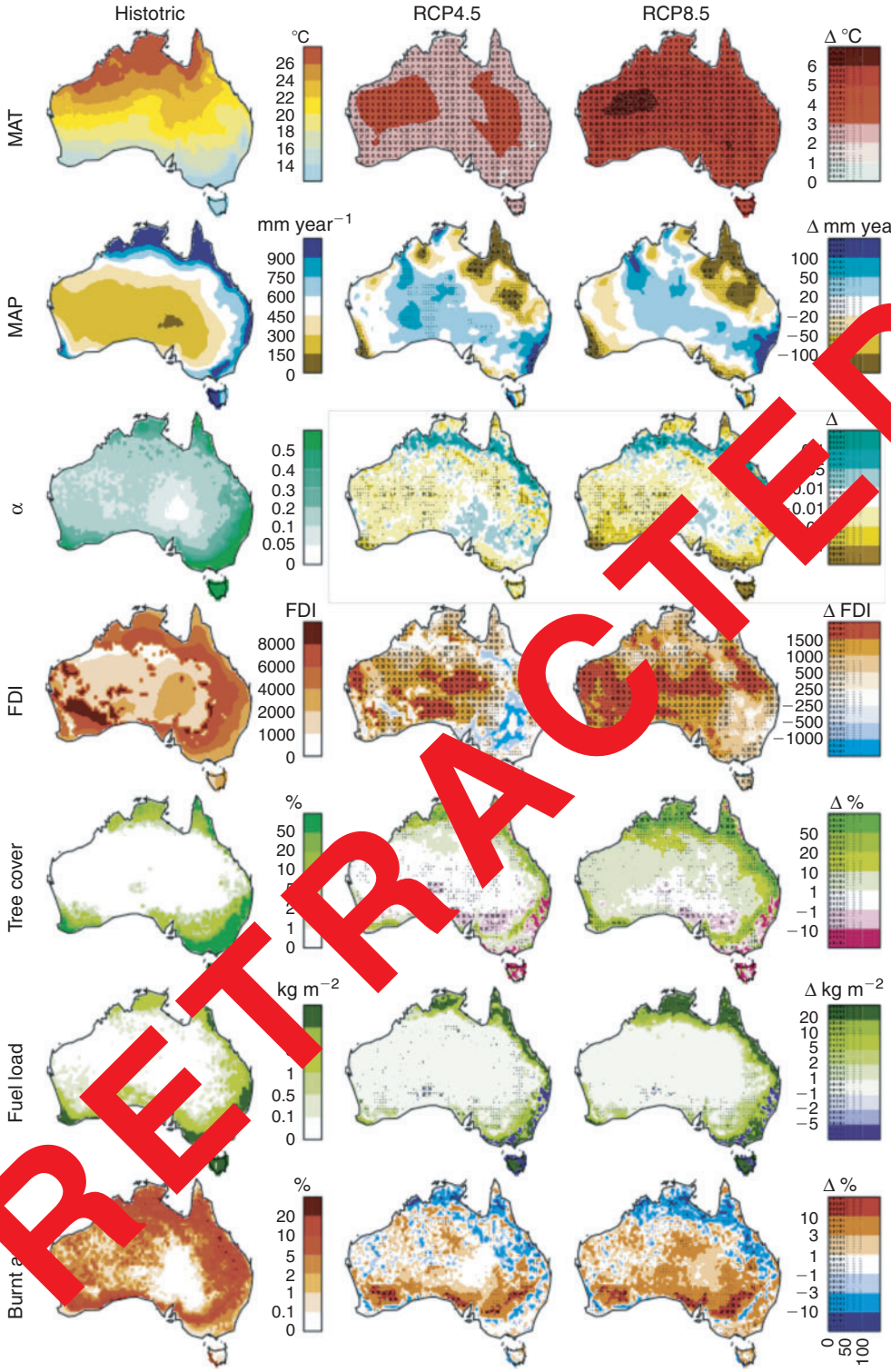

Fig. 4. Maps of the ensemble changes in climate, fire risk, vegetation and fire from the last decade of the 21st century (2090–99) for the RCP4.5 and RCP8.5 experiments compared with the historic period (1997–2006). The climate variables are mean annual temperature (MAT, °C), mean annual precipitation (MAP, mm year^{-1}) and the ratio of actual to potential evapotranspiration (α). Fire danger is represented by the McArthur cumulative fire danger index (FDI). The vegetation parameters are tree cover (%) and fuel load (kg m^{-2}), whereas fire is represented by burnt area (%). Colours show the absolute change and stippling shows the robustness of the signal (as measured by the standard deviation (s.d.) of the model results divided by the ensemble mean for each grid cell), where stippled areas indicate higher confidence in the signal.

Table 4. Summary of changes in climate, vegetation parameters and burnt area over the 21st century, based on ensemble averages of the simulations driven by the RCP4.5 and RCP8.5 climate scenarios, for Australia as a whole and for the four subregions used in this study

MAT, mean annual temperature; MAP, mean annual precipitation; α, ratio of actual to equilibrium evapotranspiration; NPP, net primary production. Total land area for each region is given in parentheses, for comparison with the values for burnt area

		MAT (°C)	MAP (mm year^{-1})	α	NPP (kg C m^{-2} year^{-1})	Tree cover (%)	Fine fuel (kg m^{-2})	Coarse fuel (kg m^{-2})	Burnt area (million km^2)
Australia	Historic	21	503	0.20	0.29	9.81	0.16	0.80	0.41
(7.94 × 10^6 km^2)	RCP4.5	24 ± 0.56	494 ± 28	0.19 ± 0.02	0.35 ± 0.03	14 ± 1.57	0.22 ± 0.02	1.50 ± 0.13	0.46 ± 5.96
	RCP8.5	25 ± 0.92	487 ± 48	0.18 ± 0.02	0.56 ± 0.07	22 ± 4.25	0.28 ± 0.05	2.10 ± 0.26	0.51 ± 11
South-east	Historic	12	832	0.58	0.78	81	1.20	12.1	0.005
(0.35 × 10^6 km^2)	RCP4.5	14 ± 0.33	786 ± 39	0.56 ± 0.02	0.97 ± 0.03	73 ± 2.59	1.46 ± 0.26	[illegible] 6.00	0.007 ± 0.11
	RCP8.5	16 ± 0.74	807 ± 75	0.48 ± 0.03	1.19 ± 0.06	74 ± 3.83	1.68 ± 0.3[illegible]	22.5[illegible]2	0.01 ± 0.31
South-west	Historic	17	421	0.26	0.37	17	0.27	0.2[illegible]	0.037
(0.44 × 10^6 km^2)	RCP4.5	20 ± 0.48	394 ± 47	0.23 ± 0.02	0.44 ± 0.04	22 ± 3.18	0.33 ± 0.0[illegible]	0.47 ± 0[illegible]	0.052 ± 0.38
	RCP8.5	22 ± 0.88	351 ± 58	0.19 ± 0.03	0.51 ± 0.10	32 ± 3.84	0[illegible] ± 0.09	[illegible]0 ± [illegible]0	0.049 ± 0.84
Central	Historic	20	251	0.11	0.14	0.81	0.02	[illegible]6	0.06
(2.18 × 10^6 km^2)	RCP4.5	23 ± 0.54	232 ± 31	0.10 ± 0.01	0.17 ± 0.03	0.63 ± 0.[illegible]	0.05 ± [illegible]01	0.002 ± 0.001	0.11 ± 2.98
	RCP8.5	25 ± 0.88	210 ± 50	0.08 ± 0.02	0.22 ± 0.06	2.62 ± 1.[illegible]	0[illegible] ± 0.02	0.003 ± 0.001	0.15 ± 4.49
North	Historic	27	1161	0.31	0.50	[illegible]6	0.22	0.40	0.08
(0.81 × 10^6 km^2)	RCP4.5	29 ± 0.57	1113 ± 82	0.33 ± 0.03	0.65 ± 0.08	[illegible] ± 9.52	0.[illegible]0	2.90 ± 1.7	0.05 ± 0.88
	RCP8.5	31 ± 1.05	1121 ± 139	0.32 ± 0.04	0.87 ± 0.13	[illegible] ± 13	0.54 [illegible]0.19	5.3 ± 3.0	0.04 ± 0.62

The continental interior, occupied by shrubland and open savanna, is projected to experience a large increase in fire over the 21st century. Burnt area increases from 0.06 × 10^6 km^2 year^{-1} in the historic simulations to 0.11 × 10^6 km^2 year^{-1} (RCP 4.[illegible]) or 0.15 × 10^6 km^2 year^{-1} (RCP8.5) by the end of the 21st c[illegible]y (Fig. 5, Table 4), representing a 78% (RCP4.5) or 142% (RCP[illegible]5) increase relative to the historic burnt area in this region. [illegible] increased temperatures and decreased precipitat[illegible]er most of this region increase fire danger (Fig. 4). [illegible]nder [illegible]esent-day conditions, low fuel loads limit burnt area in [illegible]ch c[illegible]erior; increased temperature and decreased p[illegible]ecipitat[illegible]hould fur[illegible]ther reduce vegetation productivity and [illegible]nce fuel l[illegible]. Thus, the simulated increase in fire in the i[illegible] is predomina[illegible]tly a result of the direct impacts of CO_2 on v[illegible]egetat[illegible]roductivity (Fig. 6). In the fixed-CO_2 simulations NPP is dec[illegible]ed by 13% in the RCP4.5 and 26% in the [illegible]CP8.5 simulations compared with the historic simulation, [illegible]lting [illegible]reduced fuel and a decrease in burnt area compared [illegible]e histo[illegible] period in both scenarios (Table 5; Fig. 6).

South-ea[illegible]ustralia [illegible]ome of the largest increases in fire, with [illegible]me ar[illegible] experiencing a 10–20% increase in burnt area by t[illegible]nd [illegible]the [illegible]tury in both RCP simulations (Fig. 4, Table 4). Th[illegible] increases result from a combination of increased fuel load and [illegible]eased fuel moisture (Fig. 5). The increase in fuel load is a result of CO_2 fertilisation (Fig. 6): in the fixed-CO_2 simulations, fuel load is reduced to 1.06 and 0.73 kg m^{-2} in the RCP4.5 and RCP8.5 simulations respectively, compared with 1.2 kg m^2 in the control simulation. Despite the increase in burnt area, tree cover still increases in the south-eastern interior (Fig. 4). In contrast, tree cover is reduced in forested coastal regions (from 81% in the control simulation to 73–74% in the RCP simulations, Table 4), largely owing to increases in burnt area in areas with low fire in the historic period (Fig. 4).

South-western Australia is characterised by large projected increases in fire over the 21st century (Fig. 4). Burnt area [illegible]creases fro[illegible]m 0.038 × 10^6 km^2 year^{-1} in the historic simula[illegible]ns to 0.0[illegible] × 10^6 km^2 year^{-1} (RCP4.5) and 0.049 × 10^6 km^2 y[illegible]$^{-1}$ (RC[illegible].5) (Fig. 5, Table 4), representing a 37% (RCP4.5) or 2[illegible]CP8.5) increase in the historic burnt area. There is only a small and non-robust change in fuel moisture, and the [illegible]ase in fire is almost entirely driven by an increase in fuel loads (Fig. 5) with average fuel loads increasing from 0.27 to 0.33 and 0.36 kg m^2 in RCP4.5 and RCP 8.5 respectively. This increase in fuel load is a result of CO_2 fertilisation. In the fixed-CO_2 simulations, fuel loads decreased by 0.02 kg m^2 in the RCP4.5 and 0.08 kg m^2 in the RCP8.5 simulations compared with the historic simulation (Table 5). The regional increase in fire is driven by changes in the woodland and grassland areas of the interior; fire decreases in those areas where forest replaces sclerophyll woodland (Fig. 4; Fig. 7) owing to a higher proportion of coarser fuel, which dries more slowly. Overall, tree cover in south-western Australia increases from 17% in the historic simulations to 22% in the RCP4.5 and 32% in the RCP8.5 simulations, partly owing to the conversion from sclerophyll woodland to forest but also owing to increases in woody vegetation in the interior, despite the increase in fire.

Impacts of changing fire regimes and climate on vegetation patterns

The simulated changes in fire regimes and climate produce noticeable changes in vegetation distribution by the end of the 21st century (Fig. 7). The pattern of expansion and/or contraction of major biomes is similar in the two RCP scenarios, but more exaggerated in RCP8.5. The area of grass and shrubland is reduced from 5.34 × 10^6 km^2 in the historic simulation to 4.91 × 10^6 km^2 in the RCP4.5 and 3.08 × 10^6 km^2 in the RCP8.5 simulation, equivalent to a decrease of 8 and 42% respectively. These changes largely reflect the expansion of tropical savanna in northern Australia (Fig. 7). This conversion occurs because of CO_2 fertilisation and despite small but significant increases in

burnt area: there is no southward expansion of tropical savanna in the fixed-CO_2 RCP4.5 simulations and grasslands expand in the fixed-CO_2 RCP8.5 simulations (except in the region along the north-eastern coast). Much larger increases in fire (by ~15%) cause grassland to expand into sclerophyll woodlands in southern Australia (Fig. 7), reducing the area of sclerophyll woodlands by 0.32×10^6 km^2 in RCP4.5 and 0.25×10^6 km^2 in RCP8.5. This expansion is even more pronounced in the fixed-CO_2 experiments: in the RCP8.5 simulation, for example, sclerophyll woodland barely expands beyond the area occupied by temperate forests in the present day. Thus, increased CO_2 offsets the negative impacts of increased fire on sclerophyll woodlands in southern Australia. The area of warm temperate broadleaved forest expands during the 21st century by 45 and 104% respectively in the RCP4.5 and RCP8.5 simulations. This expansion also reflects CO_2 fertilisation as the area of warm temperate broadleaved forest is reduced slightly compared with present in the fixed-CO_2 simulations (Fig. 7).

Even within regions where there is no change in biome by the end of the 21st century, the simulated changes in climate and fire regimes result in changes in the character of the vegetation (Fig. 8). Thus, areas that are characterised as tropical savanna both today and at the end of the 21st century nevertheless show an increase in tree cover. The increase in tree cover results from a large increase in the abundance of non-resprouting trees and there is a decrease in the relative importance of resprouters in these ecosystems (Fig. 8). Both the increase in tree cover and the increase in the relative importance of non-resprouters are consistent with the simulated decrease in burnt area. In areas where tropical forests persist, increased fi[illegible]s to a decrease in tree cover overall but an increa[illegible]in the [illegible]undance of resprouting trees, which partially o[illegible]s the dec[illegible]se in non-resprouting trees (Fig. 8). Again, both th[illegible]crease[illegible] tree cover and the shift in the balance [illegible]esprouting[illegible]-resprouting trees are consistent with th[illegible]hange[illegible] fire. Ar[illegible]as that persist as sclerophyll woodland [illegible]ou[illegible]eastern and south-western

Fig. 5. Factors affecting regional changes in burnt area in northern (N), central (C), south-western (SW) and south-eastern (SE) Australia. The histograms show the mean change in burnt area (%), tree cover (%), minimum fuel moisture (i.e. the mean fuel moisture during the month with the lowest overall values of fuel moisture, %), coarse fuel (kg m^{-2}) and fine fuel (kg m^{-2}) in the last decade of the 21st century (2090–99) for the RCP4.5 and RCP8.5 experiments compared with the historic period (1997–2006). The black bars show the standard deviation of the individual experiments.

Australia show an increase in tree cover despite the simulated increase in fire, and this is reflected in an increase in the importance of resprouting trees. Areas that persist as grass and shrubland nevertheless show a small CO_2-induced increase in woody cover. The increase in non-resprouting trees is greater than the increase in resprouting trees, because they have a competitive advantage over resprouters in terms of regeneration from seed in areas of low vegetation density. The incidence of fire increases but is still limited by fuel availability, and thus is not a major determinant in the balance between resprouters and non-resprouters in this ecosystem. The balance between resprouting and non-resprouting trees is affected by changes in fire regimes but is also affected by changes in other ecosystem properties. This is most clearly seen in areas that persist as temperate forests in south-eastern Australia. The decrease in tree cover in this region (Fig. 8) is largely driven by increased aridity, rather than fire. In the absence of a significant increase in fire, the relative abundance of non-re s increases because they have higher regeneration tes th non-resprouters. However, the expected impact change fire regime on the relative abundance of resprouter d non- prouters is seen in the comparison of the P4.5 and results, where the larger increase in fire i e RC 8.5 scena o results in a smaller relative increase in n- routers and a smaller relative decrease in resp uters (8).

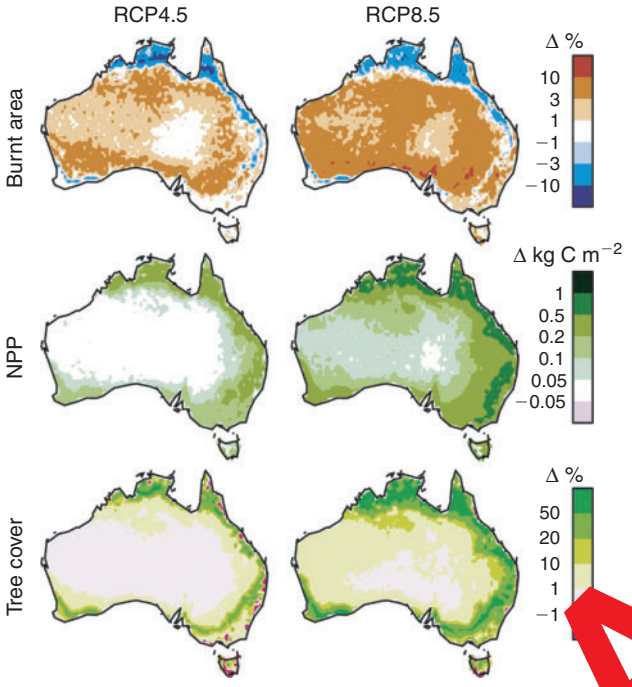

Fig. 6. Maps of the difference in burnt area (%), ne productio (NPP, kg C m^{-2}) and tree cover (%) in the last de of the st century (2090–99) between the RCP simulations with fixed and tions in which both climate and CO_2 were allo ed to positive alues therefore have the sense here of the im of CO_2 isation on the variable.

Discussi

Previous studies h uggested that the risk of fire, as measured b form of fire anger index, is likely to increase across stralia in response to projected future changes in temperature d precipi ion (Williams *et al.* 2001; Hennessy *et al.* 2005; as *et al* 07; Pitman *et al.* 2007; Fox-Hughes *et al.* 2014). Th robust increase in fire danger at the end of the 21st century in the RCP8.5 scenario over almost the entire tinent (Fig. 4). The extent of the region characterised by increased fire danger by the end of the 21st century is more limited in the RCP4.5 simulations but nevertheless most of western and central Australia shows an increase in fire danger. However, increased fire danger does not map on to changes in burnt area. Our simulations show reduced burnt area in northern Australia despite a significant and robust increase in fire danger. This reflects the fact that changes in vegetation density and in

Table 5. Summary of ch ges in egetation parameters and burnt area over the 21st century, based on ensemble averages of the simulations driven by the RCP4 d RC .5 climate scenarios but with CO_2 held constant at the 2006 level of 380.8 ppm (fixed-CO_2 experiment)

NPP, net primary production

		NPP (kg C m^{-2} $year^{-1}$)	Tree cover (%)	Fine fuel (kg m^{-2})	Coarse fuel (kg m^{-2})	Burnt area (million km^2)
Australia 4 × 1	Historic	0.29	9.81	0.16	0.80	0.41
	RCP4.5	0.26 ± 0.03	8.28 ± 0.62	0.14 ± 0.01	0.80 ± 0.11	0.36 ± 4.89
	RCP8.5	0.23 ± 0.03	6.31 ± 1.12	0.10 ± 0.01	0.48 ± 0.07	0.28 ± 6.80
South-east (0.35 × km^2)	Historic	0.78	81	1.20	12.1	0.005
	RCP4.5	0.83 ± 0.03	69 ± 1.98	1.06 ± 0.16	10.7 ± 3.20	0.004 ± 0.09
	RCP8.5	0.81 ± 0.04	56 ± 6.59	0.73 ± 0.06	0.58 ± 5.90	0.006 ± 0.27
South-west (0.44 × 10^6 km^2)	Historic	0.37	17	0.27	0.28	0.04
	RCP4.5	0.35 ± 0.04	13 ± 2.09	0.25 ± 0.03	0.36 ± 0.06	0.04 ± 0.50
	RCP8.5	0.28 ± 0.05	8.02 ± 2.19	0.19 ± 0.04	0.35 ± 0.05	0.03 ± 0.92
Central (2.18 × 10^6 km^2)	Historic	0.14	0.81	0.02	0.006	0.06
	RCP4.5	0.12 ± 0.02	0.21 ± 0.06	0.02 ± 0.01	0.003 ± 0.001	0.06 ± 1.91
	RCP8.5	0.10 ± 0.02	0.08 ± 0.04	0.01 ± 0.01	0.002 ± 0.001	0.04
North (0.81 × 10^6 km^2)	Historic	0.50	16	0.22	0.40	0.08
	RCP4.5	0.43 ± 0.06	16 ± 3.53	0.15 ± 0.05	0.93 ± 3.90	0.08 ± 0.61
	RCP8.5	0.37 ± 0.09	14 ± 5.73	0.10 ± 0.05	0.58 ± 0.33	0.07 ± 0.78

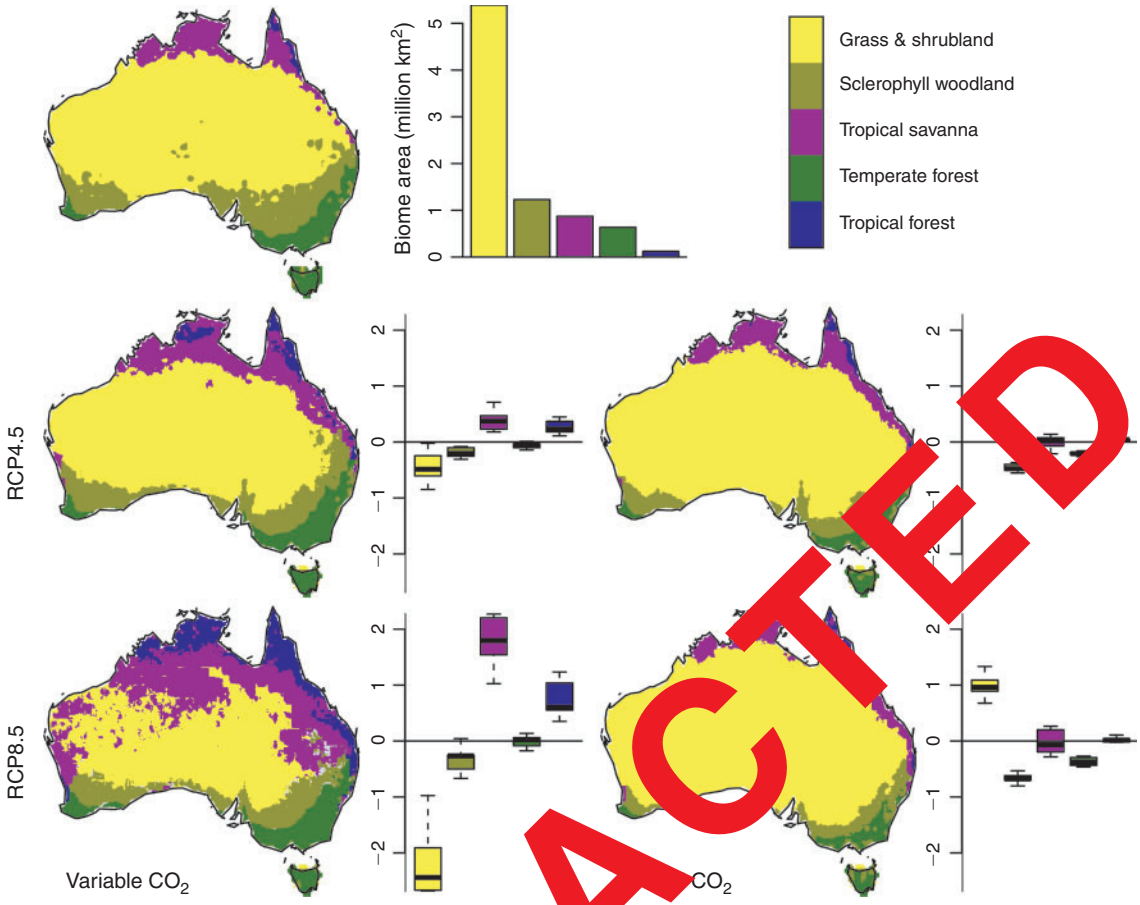

Fig. 7. Maps of the ensemble changes in veget ibution d g the last decade of the 21st century (2090–99) for the RCP4.5 and RCP8.5 experiments compared with the h ric pe d (1997–20 6). To isolate the impact of CO_2 fertilisation on the vegetation, the results for the same decade of the RC and ixed-CO_2 experiments are also shown. The simulated abundance of individual plant functional types (PFTs) was co d to maj vegetation types (biomes) using a modified version of the algorithm described in Prentice *et al.* (2011). Th ange in th a of each biome (million km^2) between the last decade of the historic period and the last decade of the 21st centur own in the box whisker plots, where the black lines shows the median value, the box shows the interquartile range and the isk how the 95% range of the model values.

the nature of the available el can gnificantly affect the spread of fire. Similarly, the area f uthern ustralia that show the largest increases in fire dang re n he areas that show the largest changes t area. e RCP4.5 scenario runs, regions in sou easte ustralia that show reduced fire danger actually show in ase burnt area. Again, the increase in burnt area in this on reflects the role of vegetation changes – in particular the i ase in fuel loads – in modulating fire regimes. Fire danger indices were developed as a management tool to predict the likelihood of fire in response to changes in fire-promoting weather conditions (McArthur 1973; Deeming *et al.* 1977; Van Wagner 1987; Matthews 2009). They are not appropriate tools to examine the consequences of long-term changes in climate, changes that impact vegetation properties directly, on fire regimes.

The direct effects of increasing CO_2 on vegetation productivity and water-use efficiency influence simulated fire regimes. CO_2 effects tend to increase fuel loads and fuel continuity in arid regions where fuel rather than climate conditions currently limits the occurrence of fire. However, in more wooded regions, CO_2 leads to increased vegetation density and this generally reduces burnt area. The role of increasing CO_2 on vegetation productivity and fuel loads has been highlighted as the dominant cause of changing fire regimes on glacial–interglacial timescales (Martin Calvo *et al.* 2014). Increased productivity and fuel loads, and increased vegetation density, have also been identified as a response to CO_2 fertilisation in simulations of 21st century changes in fire regimes and emissions made with the model LPJ-GUESS-SIMFIRE (Knorr *et al.* 2016*b*), although the impact on burnt area was not quantified. The projections of future fire regimes used in the recent Intergovernmental Panel on Climate Change (IPCC) report (Settele *et al.* 2014) were based on statistical modelling from Moritz *et al.* (2012), which cannot account for the independent effects of changes in CO_2 on fuel loads. Fire-enabled DGVMs, which explicitly simulate the impact of CO_2 on fuel loads, are more appropriate tools to examine the consequences of long-term changes in climate on fire regimes.

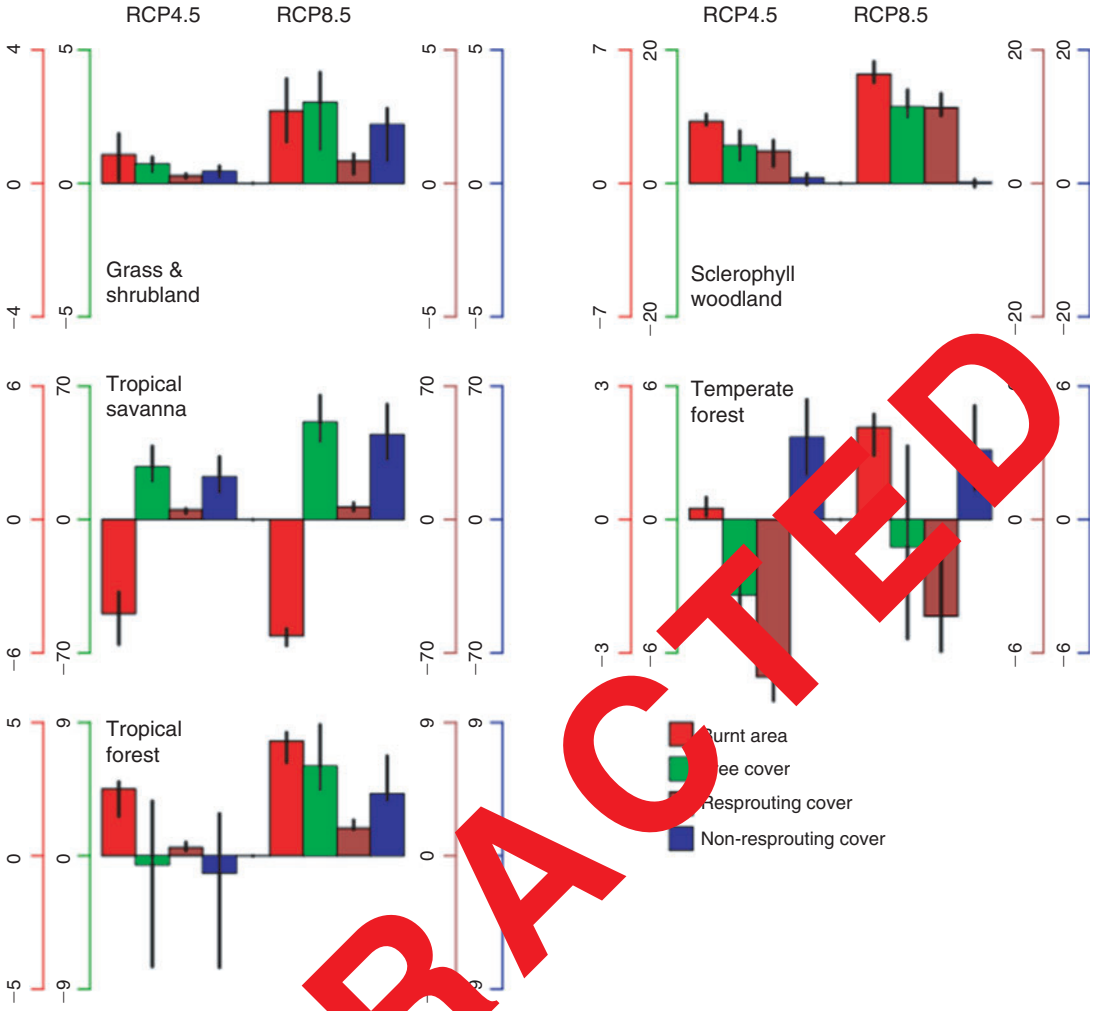

Fig. 8. Impact of changes in climate, CO_2 and fire on plant functional types (PFTs) in regions where biomes remain unchanged by the end of the 21st century in the RCP4.5 and 8.5 scenario simulations. The plots show the change in the abundance of resprouting and non-resprouting trees (%) compared with changes in burnt area (%) and tree cover (%) within each of the five major biomes: grass and shrubland, tropical savanna, tropical forest, sclerophyll woodland and temperate forest.

According to our simulations, the overall increase in burnt area over the course of the 21st century is comparatively small, with only an additional 1% of the continent burnt each year compared with today. There are, however, shifts in the spatial patterns of burning, with increased burnt area in woodland regions in the south and decreased burnt area in the north, and these shifts are likely to have important consequences on the economic impacts of fire (Ashe *et al.* 2008; Crompton and McAneney 2008; Stephenson *et al.* 2012; Hughes and Steffen 2013). Nevertheless, although the changes in fire are muted, the combined effects of changing climate, atmospheric CO_2 concentration and fire regimes have large impacts on ecosystems. According to our simulations, 22% of the continent will be affected by changes large enough to cause a shift in biome type under the RCP4.5 scenario, whereas 49% of the continent will be affected by biome shifts in the RCP8.5 scenario. The area of tropical forests increases by ~218% (648%) and the area of tropical savannas by ~45% (200%) by the end of the century in the RCP 4.5 (RCP8.5) scenario. At the same time, the area of sclerophyll woodlands decreases by ~13% (23%) and the area of grass and shrublands by ~9% (43%) by the end of the century in the RCP 4.5 (RCP8.5) scenario. Even in regions where the combined influence of climate, CO_2 and fire is insufficient to cause biome changes, there are changes in the relative abundance of different PFTs. Although we have focused on changes in tree cover and in the abundance of resprouting trees, because of the potential feedbacks between these vegetation parameters and fire, the simulations also show large shifts in the abundance of evergreen versus deciduous trees or between broadleaf and needleleaf trees in specific regions. These changes in ecosystem properties could have significant impacts on biodiversity and ecosystem services (Steffen *et al.* 2009; Booth 2012).

Human-set fires are a major component of modern-day fire regimes in many regions of the world and may affect both the type and timing of fires (Archibald *et al.* 2013). Human-set fires are a major management tool in northern Australia, for example,

and have been invoked to explain the large area burnt there annually (Murphy *et al.* 2013). However, in contrast to many other fire models, LPX-Mv1 does not include anthropogenic ignitions. Our motivation for this is that the number of ignitions is not a limiting factor on overall burnt area at a regional scale; regional analyses have shown that burnt area is strongly controlled by fuel availability and fuel moisture (Bistinas *et al.* 2014; Knorr *et al.* 2016*a*). Indeed, the apparent relationship between population density and burnt area (which forms the basis for the parameterisation of human ignitions in other fire models: Hantson *et al.* 2016) is an artefact due to the causal correlations between population density, vegetation productivity and aridity (Bistinas *et al.* 2014). Lack of anthropogenic ignitions does not explain the underestimation of burnt area in northern Australia in our simulations, which is a result of simulated fuel loads being too wet throughout the year and is not improved by increasing or changing the timing of ignitions.

The RCP4.5 and RCP8.5 scenarios represent a moderate and a high-end increase in radiative forcing over the 21st century, leading to an increase in global temperature of 1.8 ± 0.7 and 3.7 ± 1.1°C respectively by the end of the century. However, our simulations do not take into account possible increases in the frequency of lightning associated with warming temperatures and increased convection because of the large uncertainty about the quantitative relationship between these variables. Increases in the number of lightning strikes may lead to increases in ignitions, but this would not necessarily translate into an increase in fire – there is an increasing amount of evidence indicating that the number of ignitions is not the limiting factor on biomass burning globally (Bistinas *et al.* 2014; Knorr *et al.* 2016*b*). Nevertheless, changes in lightning ignitions could be important at a regional scale and it would be useful to take such changes into account. Our results involve a further simplification in that we do not include anthropogenic fire suppression or how this might change in response to the growth of population or changing patterns of human settlement. Although this decision was largely pragmatic, it also reflects a relatively simple approach to treating fire suppression in state-of-the-art models (Hantson *et al.* 2016).

The trajectory of future climate and CO_2 change is uncertain and our focus on the RCP4.5 and RCP8.5 scenarios therefore arbitrary. Furthermore, the non-negligible differences in the response of different climate models to these changes and the use of an ensemble of models does not guarantee that the average state is realistic (Tebaldi and Knutti 2007; Knutti 2010). Furthermore, LPX-Mv1 itself has regional biases in both the amount of vegetation cover (and hence fuel loads) and in the simulated burnt area under modern conditions. These biases likely affect the absolute magnitude of simulated changes during the 21st century, although they should not affect the direction and relative magnitudes of change. Thus, for many reasons, our results are indicative rather than definitive statements about the likely changes in regional fire regimes and vegetation during the 21st century across Australia. However, process-based modelling provides a tool for addressing the complexity of the interaction between vegetation and fire, and these simulations show that future fire regimes are influenced by these interactions. The projections should provide a more robust basis for developing fire management and mitigation strategies.

Conclusion

Simulations with the LPX-Mv1 DGVM show an increase in burnt area of between 12 and 24% by the end of the 21st century under the RCP4.5 and RCP8.5 scenarios. The change in burnt area is modest given the simulated changes in climate and the large increases in climate-determined 'fire risk' as measured by the McArthur Fire Danger Index. CO_2-induced changes in vegetation productivity modulate the direct climate impacts on fire regimes, leading to increased burnt area in currently fuel-limited regions but decreasing burnt area in many forested regions. Changes in fire regimes in turn affect natural ecosystems, leading to changes in the relative abundance of types of plant (grass versus trees, resprouters versus non-resprouters) within ecosystems and substantial shifts in the distribution of major vegetation types. Process-based modelling makes it possible to account for the complex two-way interactions between fire and vegetation and thus to make projections of the response of both to future climate changes. There are uncertainties associated with future climate projections and in the modelling of vegetation and fire responses to climate change. Nevertheless, the simulations presented here offer a firmer foundation for understanding future climate impacts on fire and vegetation than approaches based on extrapolation from modern climate–fire relationships.

Acknowledgements

We acknowledge the World Climate Research Program's Working Group on Coupled Modelling, which is responsible for CMIP, and the climate modelling groups for producing and making available their model output. (For CMIP, the US Department of Energy's Program for Climate Model Diagnosis and Intercomparison provides coordinating support and led development of software infrastructure in partnership with the Global Organisation for Earth System Science Portals.) The analyses and figures are based on data archived by 18 June 2013. DIK was supported by an iMQRES scholarship at Macquarie University and postdoctoral funding from the University of Reading. We thank Colin Prentice for comments on the draft manuscript.

References

Archibald S, Lehmann CER, Gómez-Dans JL, Bradstock RA (2013) Defining pyromes and global syndromes of fire regimes. *Proceedings of the National Academy of Sciences of the United States of America* **110**, 6442–6447. doi:10.1073/PNAS.1211466110

Ashe B, McAneney KJ, Pitman AJ (2009) The total cost of fire in Australia. *Journal of Risk Research* **12**, 121–136. doi:10.1080/13669870802648528

Barrett DJ (2001) NPP multi-biome: VAST calibration data, 1965–1988, R1. Available at http://daac.ornl.gov/cgi-bin/dsviewer.pl?ds_id=576 [Verified 16 August 2016]

Bartholomé EM, Belward AS (2005) GLC2000: a new approach to global land-cover mapping from Earth observation data. *International Journal of Remote Sensing* **26**, 1959–1977. doi:10.1080/01431160412331291297

Bistinas I, Harrison SP, Prentice IC, Pereira JMC (2014) Causal relationships versus emergent patterns in the global controls of burnt area. *Biogeosciences* **11**, 5087–5101. doi:10.5194/BG-11-5087-2014

Booth T (2012) Biodiversity and climate change adaptation in Australia: strategy and research developments. *Advances in Climate Change Research* **3**, 12–21. doi:10.3724/SP.J.1248.2012.00012

Bradstock RA (2008) Effects of large fires on biodiversity in south-eastern Australia: disaster or template for diversity? *International Journal of Wildland Fire* **17**, 809–822. doi:10.1071/WF07153

Bradstock RA, Williams RJ, Gill AM (Eds) (2012) 'Flammable Australia: fire regimes, biodiversity and ecosystems in a changing world.' (CSIRO Publishing: Melbourne)

Brovkin V, van Bodegom PM, Kleinen T, Wirth C, Cornwell WK, Cornelissen JHC, Kattge J (2012) Plant-driven variation in decomposition rates improves projections of global litter stock distribution. *Biogeosciences* **9**, 565–576. doi:10.5194/BG-9-565-2012

Clarke PJ, Lawes MJ, Midgley JJ, Lamont BB, Ojeda F, Burrows GE, Enright NJ, Knox KJE (2013) Resprouting as a key functional trait: how buds, protection and resources drive persistence after fire. *New Phytologist* **197**, 19–35. doi:10.1111/NPH.12001

Collins M, Knutti R, Arblaster J, Dufresne JL, Fichefet T, Friedlingstein P, Gao X, Gutowski WJ, Johns T, Krinner G, Shongwe M, Tebaldi C, Weaver AJ, Wehner M (2013) Long-term climate change: projections, commitments and irreversibility. In 'Climate change 2013: the physical science basis. Contribution of Working Group I to the Fifth Assessment Report of the Intergovernmental Panel on Climate Change'. (Eds TF Stocker, D Qin, G-K Plattner, M Tignor, SK Allen, J Doschung, A Nauels, Y Xia, V Bex, PM Midgley) pp. 1029–1136. (Cambridge University Press: Cambridge, UK and New York, NY)

Crompton RP, McAneney KJ (2008) Normalised Australian insured losses from meteorological hazards: 1967–2006. *Environmental Science & Policy* **11**, 371–378. doi:10.1016/J.ENVSCI.2008.01.005

Deeming JE, Burgan RE, Cohen JD (1977) The national fire-danger rating system – 1978. USDA Forest Service, Intermountain Forest and Range Experiment Station, General Technical Report INT-39. (Ogden, UT).

DeFries R, Hansen MC (2009) ISLSCP II continuous fields of vegetation cover, 1992–1993. In 'ISLSCP initiative II collection, data set' (Eds FG Hall, G Collatz, B Meeson, S Los, E Brown De Colstoun, D Landis) (Oak Ridge National Laboratory Distributed Active Archive Cente[illegible] Ridge, TN) Available at https://daac.ornl.gov/ISLSCP_II/guide[illegible] continuous_fields_xdeg.html [Verified 16 August 2016]

Fox-Hughes P, Harris R, Lee G, Grose M, Bindoff N (2014) Future [illegible] danger climatology for Tasmania, Australia, using a [illegible] scaled regional climate model. *International Jo[illegible]l of Wildland Fir[illegible]* **23**, 309–321. doi:10.1071/WF13126

Geng S, Auburn JS, Brandstetter E, Li B (1988) A[illegible]m to s[illegible]ate meteorological variables: documentati[illegible]or SIMF[illegible]FO. Agronomy Progress Report 204. (Department [illegible]gronomy and [illegible]ge Science, University of California, Davis: [illegible])

Giglio L, Randerson JT, van der Werf G[illegible]013) Analysis of daily, monthly, and annual burn[illegible] area using the [illegible]rth-generation Global Fire Emissions Databa[illegible]GFED4). *Journal of Geophysical Research. Biogeosciences* **118**[illegible]–328[illegible].10.1002/JGRG.20042

Gill AM (2012) Bushfire[illegible] diversit[illegible]in southern Australian forests. In 'Flammable Australia[illegible] regi[illegible] biodiversity and ecosystems in a changin[illegible]'. (Eds [illegible]adstock, RJ Williams, AM Gill) pp. 235[illegible] (CS[illegible]O Publishin[illegible]. Melbourne).

Groves R[illegible]1994)[illegible]ian vegetation.' (Cambridge University Press: Cambri[illegible])

Hantson S, Al[illegible]A, Harrison SP, Kelley DI, Prentice IC, Rabin SS, Archibald S, [illegible]illot F, Arnold SR, Artaxo P, Bachelet D, Ciais P, Forrest M, Friedlingstein P, Hickler T, Kaplan JO, Kloster S, Knorr W, Lasslop G, Li F, Melton JR, Meyn A, Sitch S, Spessa A, van der Werf GR, Voulgarakis A, Yue C (2016) The status and challenge of global fire modelling. *Biogeosciences Discussions* **13**, 3350–3375. doi:10.5194/BG-2016-17

Harris I, Jones PD, Osborn TJ, Lister DH (2013) Updated high-resolution grids of monthly climatic observations – the CRU TS3.10 dataset. *International Journal of Climatology*. doi:10.1002/JOC.3711

Harrison SP, Marlon JR, Bartlein PJ (2010) Fire in the Earth system. In 'Changing climates, Earth systems and society'. (Ed. J Dodson) pp. 21–48. (Springer: Dordrecht, the Netherlands)

Hartmann DL, Klein Tank AMG, Rusticucci M, Alexander LV, Brönnimann S, Charabi Y, Dentener FJ, Dlugokencky EJ, Easterling DR, Kaplan A, Soden BJ, Thorne PW, Wild M and Zhai PM (2013) Observations: atmosphere and surface. In 'Climate change 2013: the physical science basis. Contribution of Working Group I to the Fifth Assessment Report of the Intergovernmental Panel on Climate Change' (Eds TF Stocker, D Qin, G-K Plattner, M Tignor, SK Allen, J Boschung, A Nauels, Y Xia, V Bex and PM Midgley) Cambridge University Press, Cambridge, United Kingdom and New York, NY, USA. doi:10.1017/CBO9781107415324

Haverd V, Raupach MR, Briggs PR, Canadell JG, Davis SJ, Law RM, Meyer CP, Peters GP, Pickett-Heaps C, Sherman B (2013) The Australian terrestrial carbon budget. [illegible]*ciences* **10**, 851–869. doi:10.5194/BG-10-851-2013

Hennessy K, Bathols C, Lucas N, Nie[illegible]s J, Suppia[illegible] Ricketts J (2005) Climate change impacts on fire-weat[illegible] south-e[illegible] Australia. Technical Report. Available at h[illegible]//eprints.[illegible]d.es[illegible]nimelb.edu.au/244/ [Verified 16 August 201[illegible]

Higuera PE, Abatzoglo[illegible]. Litt[illegible]S, Morgan P (2015) The changing strength and nature of[illegible]ate rel[illegible]onships in the northern Rocky Mountains, US[illegible]1902–2[illegible] *PLoS[illegible]e* **10**(6), e0127563. doi:10.1371/JOURNAL.[illegible]NE.0127563

Hughes L, St[illegible]. (2013) Be prep[illegible]red: climate change and the Australian bushfire threat[illegible]ate Council. Available at http://www.climatecouncil.org.au/uploads[illegible]7d19c0ab18366cfbf7b9f6235ef7c.pdf [Verified [illegible]gust 2016]

[illegible]nay E, Kanamitsu M, Kistler R, Collins W, Deaven D, Gandin L, Iredell M[illegible]ha S, White G, Woollen J, Zhu Y, Leetmaa A, Reynolds R, Chelli[illegible]M, Ebisuzaki W, Higgins W, Janowiak J, Mo KC, [illegible]ele[illegible]C, Wang J, Jenne R, Joseph D (1996) The NCEP/NCAR 40-[illegible]reanalysis project. *Bulletin of the American Meteorological Society* **77**, 437–471. doi:10.1175/1520-0477(1996)077<0437:[illegible]NYRP>2.0.CO;2

Kelley DI, Prentice IC, Harrison SP, Wang H, Simard M, Fisher JB, Willis KO (2013) A comprehensive benchmarking system for evaluating global vegetation models. *Biogeosciences* **10**, 3313–3340. doi:10.5194/BG-10-3313-2013

Kelley DI, Harrison SP, Prentice IC (2014) Improved simulation of fire–vegetation interactions in the Land surface Processes and eXchanges Dynamic Global Vegetation Model (LPX-Mv1). *Geoscientific Model Development* **7**, 2411–2433. doi:10.5194/GMD-7-2411-2014

Kirtman B, Power SB, Adedovin JA, Boer GJ, Bojariu R, Camilloni I, Doblas-Reyes FJ, Fiore AM, Kimoto M, Meehl GA, Prather M, Sarr A, Schar C, Sutton R, van Oldenburgh GJ, Vecchi G, Wang HJ (2013) Near-term climate change: projections and predictability. In 'Climate change 2013: the physical science basis. Contribution of Working Group I to the Fifth Assessment Report of the Intergovernmental Panel on Climate Change'. (Eds TF Stocker D Qin, G-K Plattner, M Tignor, SK Allen, J Doschung, A Nauels, Y Xia, V Bex, PM Midgley) pp. 953–1028. (Cambridge University Press: Cambridge, UK and New York, NY)

Knorr W, Kaminski T, Arneth A, Weber U (2014) Impact of human population density on fire frequency at the global scale. *Biogeosciences* **11**, 1085–1102. doi:10.5194/BG-11-1085-2014

Knorr W, Arneth A, Jiang L (2016*a*) Demographic controls of future global fire risk. *Nature Climate Change* . doi:10.1038/NCLIMATE2999

Knorr W, Jiang L, Arneth A (2016*b*) Climate, CO_2, and demographic impacts on global wildfire emissions. *Biogeosciences* **13**, 267–282. doi:10.5194/BG-13-267-2016

Knutti R (2010) The end of model democracy? *Climatic Change* **102**, 395–404. doi:10.1007/S10584-010-9800-2

Krawchuk MA, Moritz MA, Parisien M-A, Van Dorn J, Hayhoe K (2009) Global pyrogeography: the current and future distribution of wildfire. *PLoS One* **4**, e5102. doi:10.1371/JOURNAL.PONE.0005102

Lawes MJ, Adie H, Russell-Smith J, Murphy BP, Midgley JJ (2011) How do small savanna trees avoid stem mortality by fire? The roles of stem diameter, height and bark thickness. *Ecosphere* **2**, doi:10.1890/ES10-00204.1

Lucas C, Hennessy K, Mills G, Bathols J (2007) Bushfire weather in south-east Australia: recent trends and projected climate change impacts. Available at http://www.climateinstitute.org.au/verve/_resources/full-reportbushfire.pdf [Verified 16 August 2016]

Martin Calvo M, Prentice IC, Harrison SP (2014) Climate versus carbon dioxide controls on biomass burning: a model analysis of the glacial–interglacial contrast. *Biogeosciences* **11**, 6017–6027. doi:10.5194/BG-11-6017-2014

Matthews S (2009) A comparison of fire danger rating systems for use in forests. *Australian Meteorological and Oceanographic Journal* **58**, 41–48.

McArthur AG (1966) 'Weather and grassland fire behaviour.' (Forestry and Timber Bureau, Department of National Development, Commonwealth of Australia: Canberra)

McArthur AG (1967) 'Fire behaviour in eucalypt forests.' (Forestry and Timber Bureau: Canberra).

McArthur AG (1973) Grassland Fire Danger Meter Mk IV. Bush Fire Council of NSW officer training module CL/4 – Fire behaviour, second edition. Grasslands FDIs – fire behavior relationships. Available at http://www.firebreak.com.au/grass-behave.html [Verified 16 August 2016]

Michalon N, Nassif A, Saouri T, Royer JF, Pontikis CA (1999) Contribution to the climatological study of lightning. *Geophysical Research Letters* **26**, 3097–3100. doi:10.1029/1999GL010837

Moritz MA, Parisien M-A, Batllori E, Krawchuk MA, Van Dorn J, David J, Ganz DJ, Hayhoe K (2012) Climate change and disruptions to global fire activity. *Ecosphere* **3**, 49. doi:10.1890/ES11-00345.1

Murphy BP, Bradstock RA, Boer MM, Carter J, Cary GJ, Cochrane MA, Fensham RJ, Russell-Smith J, Williamson GJ, Bowman DMJS (2013) Fire regimes of Australia: a pyrogeographic model system. *Journal of Biogeography* **40**, 1048–1058. doi:10.1111/JBI.12065

Noble IR, Bary GAA, Gill AM (1980) McArthur's fi[illegible]ange [illegible]eters expressed as equations. *Australian Journal of E[illegible]ry* **5**, [illegible] doi:10.1111/J.1442-9993.1980.TB01243.X

Pitman AJ, Narisma GT, McAneney J (2007) Th[illegible]pact of c[illegible]te change on the risk of forest and grassland fires in A[illegible]alia. *Climatic [illegible]ge* **84**, 383–401. doi:10.1007/S10584-007-92[illegible]

Prentice IC, Kelley DI, Foster PN, Friedlingstein [illegible]rrison SP, Bartlein PJ (2011) Modelling fire and [illegible] terrestrial car[illegible]balance. *Global Biogeochemical Cycles* **25**, G[illegible]005. doi:10.1029/2010GB003906

Price C, Rind D (1994) Poss[illegible]impli[illegible]ns of global climate change on global lightning distributio[illegible]n[illegible]equencies. *Journal of Geophysical Research* **99**, 10823–10831. d[illegible]1029[illegible]D00019

Romps DM, Seeley[illegible]laro D, M[illegible]J (2014) Projected increase in lightning stril[illegible]n the [illegible]ited States [illegible]e to global warming. *Science* **346**, 851–854. e[illegible]0.112[illegible]ICE.1259100

Rothermel RC ([illegible]mather[illegible]ical model for predicting fire spread in wildland fuels. [illegible]A Forest Service Intermountain Forest and Range Experiment Station[illegible]arch Paper INT-RP-115. (Ogden, UT)

Ruesch A, Gibbs HK (2008) New IPCC Tier-1 global biomass carbon map for the year 2000. Available from http://cdiac.esd.ornl.gov/epubs/ndp/global_carbon/carbon_documentation.html [Verified 8 August 2016]

Russell-Smith J, Yates CP, Whitehead PJ, Smith R, Craig R, Allan GE, Thackway R, Frakes I, Cridland S, Meyer MCP, Gill AM (2007) Bushfires 'Down Under': patterns and implications of contemporary Australian landscape burning. *International Journal of Wildland Fire* **16**, 361–377. doi:10.1071/WF07018

Settele J, Scholes R, Betts R, Bunn S, Leadley P, Nepstad D, Overpeck JT, Taboada MA (2014) Terrestrial and inland water systems. In 'Climate change 2014: impacts, adaptation, and vulnerability. Part A: global and sectoral aspects'. (Eds CB Field, VR Barros, DJ Dokken, KJ Mach, MA Mastrandrea, TE Bilir, M Chatterjee, KL Ebi, YO Estrada, RC Genova, B Girma, ES Kissel, AN Levy, S MacCracken, PR Mastrandrea, LL White) pp. 271–359. (Cambridge University Press: Cambridge, UK and New York, NY).

Sitch S, Smith B, Prentice IC, Arneth A, Bo[illegible]au A, [illegible]er W, Kaplan JO, Levis S, Lucht W, Sykes MT, Th[illegible]ke K, Ver[illegible]ky S (2003) Evaluation of ecosystem dynamics, pla[illegible]ography[illegible]d terrestrial carbon cycling in the LPJ dyna[illegible] global [illegible]tatio[illegible]odel. *Global Change Biology* **9**, 161–185. [illegible]10.1046/J.1365[illegible].2003.00569.X

Steffen W, Burbidge AA, Hug[illegible]L, Kit[illegible]g R, Lindenmayer D, Musgrave W, Stafford Smith M, Wer[illegible]009) 'A[illegible]tralia's biodiversity and climate change: a str[illegible]gic asse[illegible]nt of [illegible]vulnerability of Australia's biodiversity to cl[illegible]e change.' ([illegible]ublishing: Melbourne)

Stephenson C, H[illegible]Betts R (201[illegible]) Estimating the economic, social and environ[illegible]ental [illegible]cts of wildfires in Australia. *Environmental Hazards* **12**, 93–111. do[illegible]1080/17477891.2012.703490

Sturma[illegible]pper NJ (2005) 'The weather and climate of Australia and N[illegible]Zealand', 2nd edn. (Oxford University Press: Oxford, UK)

Tayl[illegible]KE, Stouff[illegible]J, Meehl GA (2012) An overview of CMIP5 and the e[illegible]imental d[illegible]gn. *Bulletin of the American Meteorological Society* **93**, [illegible]498[illegible]10.1175/BAMS-D-11-00094.1

Tebaldi C, [illegible]tti R (2007) The use of the multimodel ensemble in [illegible]obabilistic climate projections. *Philosophical Transactions of the [illegible]ociety A* **365**, 2053–2075. doi:10.1098/RSTA.2007.2076

[illegible]onicke K, Venevsky S, Sitch S, Cramer W (2001) The role of fire disturbance for global vegetation dynamics: coupling fire into a Dynamic Global Vegetation Model. *Global Ecology and Biogeography* **10**, 661–677. doi:10.1046/J.1466-822X.2001.00175.X

van Vuuren DP, Edmonds J, Kainuma M, Riahi K, Thomson A, Hibbard K, Hurtt GC, Kram T, Krey V, Lamarque J-F, Masui T, Meinshausen M, Nakicenovic N, Smith SJ, Rose SK (2011) The representative concentration pathways: an overview. *Climatic Change* **109**, 5–31. doi:10.1007/S10584-011-0148-Z

Van Wagner CE (1987) Development and structure of the Canadian Forest Fire Weather Index System. Canadian Forestry Service, Forestry Technical Report 35. (Ottawa, ON)

Williams A, Karoly D, Tapper NJ (2001) The sensitivity of Australian fire danger to climate change *Climatic Change* **49**, 171–191. doi:10.1023/A:1010706116176

Williams ER (1992) The Schumann resonance: a global tropical thermometer. *Science* **256**, 1184–1187. doi:10.1126/SCIENCE.256.5060.1184

Williams RJ, Bradstock RA, Cary GJ, Enright NJ, Gill AM, Liedloff A, Lucas C, Whelan RJ, Andersen AN, Bowman DMJS, Clarke PJ, Cook GD, Hennessy K, York A (2009) 'Interactions between climate change, fire regimes and biodiversity in Australia: a preliminary assessment.' (Department of Climate Change and Department of the Environment, Water, Heritage and the Arts: Canberra)